Proceedings of the
2007 IEEE Intelligent Vehicles Symposium
Istanbul, Turkey, June 13-15, 2007

Geometric and Statistic Constraints in Dynamic Re-Orientation of On-Board Camera: Inherent Vanishing Points

Lin MA[1,*], *Student Member, IEEE*, Nan-Ning ZHENG[1], *Fellow, IEEE*,
Fan Mu[1], Dong Yi[1], Hong Cheng[1], and Yongjian He[1,2]

1. Institute of Artificial Intelligence and Robotics, Xi'an Jiaotong University, Xi'an, 710049, P.R.China.
2. Xi'an Communication Institute, Xi'an, 710106, P.R.China.
LinMa@ieee.org, nnzheng@aiar.xjtu.edu.cn

***Abstract*— This paper investigates the stochastic projective properties of natural line segments in highway scenes for the purpose of dynamically re-orientating the on-board camera. We demonstrate there are geometric and statistic constraints on the projection of such line segments. A new concept of *Inherent Vanishing Points* associated with land vehicle boards was employed to relate to the observed line segments and rotation matrix. We show how these constraints greatly simplify the re-orientation of the on-board camera. We validate a dynamic re-orientation algorithm based on these constraints with a real image sequence. Compared with the techniques based on static calibration fields, the method based on our proposed statistical constraints is effective, stable, and easy to use.**

I. INTRODUCTION

Camera calibration is a necessary step in 3D reconstruction in order to extract metric information from 2D images. Therefor, on-board camera calibration is an important task for driver assistant or autonomous vision systems. Conventionally, ignoring the specific property of motion on the road, a man-made pattern or specially-made landmark is used for calibration in a static situation. Ernst[1] painted a calibration field on a piece of road, then used the points of interest to calibrate both intrinsic and extrinsic camera parameters.Wang and Tsai[2] employed a hexagon in their approach. In Bucher[3], two well-arranged parallel lines on the world plane were used.

Wang[4] considered that intrinsic camera calibration is required only once for these kinds of applications, but extrinsic camera parameters have to be calibrated many times, and even constantly over extended operating periods. In his approach for calibrating extrinsic camera parameters, a simple and analytical procedure was suggested. But Wang's method employed a group of known calibration points, which make it ineffective when land vehicle motion is taken into account.

However, the approaches mentioned above stand on the same weak presumption that the vertical axis of the reference coordinate of the land vehicle body is perpendicular with the ground plane both in static and dynamic situations. Furthermore, these approaches avoided the problem of how to determine the frontage of the vehicle in practice.

In fact, the 3D reconstruction process might be possible to implement even when the vehicle dynamic is severe There is no change in the intrinsic parameters when it is in motion. But a series of problems about relative orientation parameters must be reconsidered as follows:

- The inclination angle between the local ground plane and the image plane will change with the change in velocity of vehicle[5][6]. This would lead to a slight dynamic bias in the inclination angle. As is already known, the higher the vehicle speed, the farther the necessary look-ahead distance. As a result, a serious error would occur by triangulation in the 3D reconstruction process when the vehicle is driven at high speed.
- It is almost impossible to determine the frontage of the vehicle precisely in a static situation. There is no visible and accurate reference for the longitude axes of land vehicles; besides, the reference orientation would be changed slightly in maintenance every time. So, the definition of *frontage* is fuzzy when a land vehicle is motionless. A possible reference method would be to drive the vehicle along a long and straight line to define the reference orientation, but the error boundary of this definition is uncertain. Also, sequentially, the error of calibration result is difficult to control.

Due to the requirement that the reconstruction must work for long distances during fast movement, the dynamic re-orientation process of the on-board camera is necessary. If the camera never moved relative to vehicle after installation, then it would be easy to refine the translation vector with the re-calibrated rotation matrix. But for refining the rotation parameters, a group of reliable constraints must be found in the vehicle driving process.

Based on above facts, the primary difficulties of dynamic re-orientation for the on-board camera are as follows:

- **Uncertainty of scene content**
  The on-board camera is moving relative to the road scenes, and the view field is highly uncertain. There is no certain reference feature for parameter calibration.
- **Changeability of the pose parameter**

*This work was supported by the grants from the National Basic Research Program of China (973 Program) (No. 2006CB708303), the National High Technology Research and Development Program of China (863 Program) (No. 20060101Z1059) and National Key Technologies Research and Development Program of China (No. 2006BAK31B04).

The pose parameter will change as the velocity of vehicle changes, besides the bumping effect.

- **Low accuracy of the data**
  Generally, the look-ahead distance is far in high speed driving. Furthermore, for real-time processing, the resolution power of the camera is limited. These lead to a low accuracy of the data.

Accordingly, we investigated the constraints between the reference coordinate and surrounding road scenes, and suggested an effective statistic work frame for dynamic reorientation based on these constraints. It overcomes the drawbacks in the work of Ma *et al.*[7], which are too dependent on snaking driving.

In section II, a new concept of *Inherent Vanishing Points* associated with the land-vehicle board is introduced, and the relationship between these points and the rotation matrix is demonstrated. In section III we analyze the stochastic processes in vehicle motion and lead the estimation formulas of the statistic features. In section IV we show the results of our experiments. Section V draws some conclusions.

II. Inherent Vanishing Points

The projection of the land vehicle board orientation is examined in this section. We start with the notation used in this paper.

A. Notation

When several different coordinate systems are considered at the same time, it is convenient to follow Craig[8] and Firsyth[9], and denote by ${}^{F}P$ (resp. ${}^{F}v$) the coordinate vector of the point P (resp. vector v) in the frame F–that is

$$ {}^{F}P = {}^{F}\overrightarrow{OP} = \begin{pmatrix} x \\ y \\ z \end{pmatrix} \Longleftrightarrow \overrightarrow{OP} = x\boldsymbol{i} + y\boldsymbol{j} + z\boldsymbol{k} \quad . \tag{1} $$

In this paper, we consider four coordinate systems: the 2D image plane frame (Π'), the 3D camera frame (C), 3D reference frame associated with vehicle board (B), and the 3D world frame (W).

$$ \begin{aligned} (\Pi') &= (O_{\Pi'}, \boldsymbol{i}_{\Pi'}, \boldsymbol{j}_{\Pi'}) \quad ; \\ (C) &= (O_C, \boldsymbol{i}_C, \boldsymbol{j}_C, \boldsymbol{k}_C) \quad ; \\ (B) &= (O_B, \boldsymbol{i}_B, \boldsymbol{j}_B, \boldsymbol{k}_B) \quad ; \\ (W) &= (O_W, \boldsymbol{i}_W, \boldsymbol{j}_W, \boldsymbol{k}_W) \quad . \end{aligned} \tag{2} $$

We use homogeneous coordinates to represent points, vectors, and planes. A pixel point (u,v) in image plane Π' is represented as a vector $\boldsymbol{p} = [u, v, 1]^T$. A 3D space point P is represented in the world frame as ${}^{W}P = [{}^{W}X, {}^{W}Y, {}^{W}Z, 1]^T$, in the reference frame as ${}^{B}P = [{}^{B}X, {}^{B}Y, {}^{B}Z, 1]^T$, and in the on-board camera frame as ${}^{C}P = [{}^{C}x, {}^{C}y, {}^{C}z, 1]^T$.

As shown in figure1, we use a pinhole camera model in this paper: that means the following equation is satisfied[9]

$$ \boldsymbol{p} = \frac{1}{{}^{c}z} \mathcal{K} \begin{pmatrix} {}^{C}_{B}\mathcal{R} & \boldsymbol{t} \end{pmatrix} {}^{B}\boldsymbol{P} \tag{3} $$

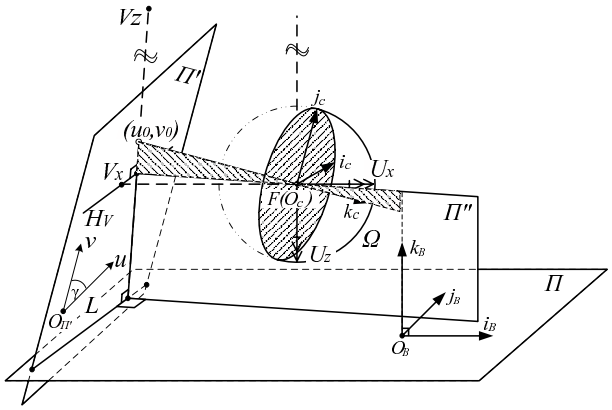

Fig. 1. On-Board Camera Model

where

$$ \mathcal{K} \stackrel{def}{=} \begin{pmatrix} \alpha & -\alpha\cot\gamma & u_0 \\ 0 & \beta/\sin\gamma & v_0 \\ 0 & 0 & 1 \end{pmatrix} \quad , $$

is called the camera intrinsic matrix, ${}^{c}z$ is the depth of point ${}^{C}P$ in camera frame, (u_0, v_0) are the coordinates of the principal point, α and β the scale factors in image u and v axes, and γ is the angle between the two image axes u and v. $\begin{pmatrix} {}^{C}_{B}\mathcal{R} & \boldsymbol{t} \end{pmatrix}$ is called the camera extrinsic matrix, ${}^{C}_{B}\mathcal{R}$ is the rotation matrix, and $\boldsymbol{t} = {}^{C}\boldsymbol{O}_B$ is the translation vector.

B. Inherent Vanishing Points and Rotation Matrix of the On-Board Camera

Definition 2.1 (Inherent Vanishing Points):
The point $V_X = [u_X, v_X, 1]^T$ in the on-board camera image plane Π' is called the Inherent Vanishing Point associated with the X_B axes, if all 3D parallel lines with orientation $\mathbf{i}_B$ project to converging lines with intersections at point V_X in image plane Π'.

Vector $\mathbf{i}_B$ is also called the corresponding vector of vanishing point V_X, and the orientation of $\mathbf{i}_B$ is called the corresponding orientation of V_X.

Similarly, $V_Y = [u_Y, v_Y, 1]^T$ and $V_Z = [u_Z, v_Z, 1]^T$ are respectively called Inherent Vanishing Points associated with the Y_B axes and Z_B axes. Vectors $\mathbf{j}_B$ and $\mathbf{k}_B$ are respectively called the corresponding vectors of vanishing points V_Y and V_Z.

V_X, V_Y, and V_Z are called by a joint name: *Inherent Vanishing Points of the On-Board Camera*.

According to the definition 2.1, the 3D orientations corresponding to Inherent Vanishing Points are respectively parallel to the relative axes. Therefore, the corresponding unit normal vectors of these Inherent Vanishing Points are the column vectors of the rotation matrix[9].

$$ {}^{C}_{B}\mathcal{R} = \begin{pmatrix} {}^{C}\boldsymbol{i}_B & {}^{C}\boldsymbol{j}_B & {}^{C}\boldsymbol{k}_B \end{pmatrix} \tag{4} $$

Thus, the problem of determining of the camera rotation matrix relative to the reference frame is translated into a new problem to estimate the Inherent Vanishing Points or their corresponding orientations.

However, as mentioned above, the view field of the on-board camera is highly uncertainty. There is no method to estimate the Inherent Vanishing Points in a single image. For this reason, we establish the statistic corresponding relationship between image features and Inherent Vanishing Points by taking into account the constraints in the vehicle motion process.

III. Basic Constraints in Vehicle Motion

In this section, we examine the statistic vision information associated with the orientation of the land vehicle board. When considering a land-vehicle driving on a highway, in general, the vehicle motion must satisfy two classification constraints correlated with the road surface and road boundaries. At the same time, we limited singularly extreme situations that would not appear in our permission application conditions, such as a road segment with an excess transect gradient.

A. Some Concepts about Road Surface

Assume that the real ground surface in the world frame is represented as

$$\Sigma: \quad {}^{W}Z = h({}^{W}X, {}^{W}Y) \tag{5}$$

If we smooth Σ by a window h with scale ε the same as the vehicle tread width, a new surface will be obtained as

$$\begin{aligned}\overline{\Sigma}: \quad {}^{W}Z &= \overline{h}({}^{W}X, {}^{W}Y) \\ &= \iint w_{\varepsilon}(s-{}^{W}X, t-{}^{W}Y)\cdot h(s,t)\,ds dt \ , \end{aligned} \tag{6}$$

where

$$h(x,y) = \begin{cases} \dfrac{1}{\varepsilon^2} & abs(x) \le \dfrac{\varepsilon}{2}, abs(y) \le \dfrac{\varepsilon}{2} \\ 0 & abs(x) > \dfrac{\varepsilon}{2}, abs(y) > \dfrac{\varepsilon}{2} \end{cases} .$$

If ${}^{W}\overline{h}_X$ and ${}^{W}\overline{h}_Y$, the derivative of $\overline{h}$, is continuous at point $({}^{W}X, {}^{W}Y)$, we could obtain $\boldsymbol{n}_{\overline{\Sigma}}$, the normal of surface $\overline{\Sigma}$ at point $({}^{W}X, {}^{W}Y, {}^{W}Z)$, which is represented in the world frame as

$${}^{W}\boldsymbol{n}_{\overline{\Sigma}} = [{}^{W}\overline{h}_X, {}^{W}\overline{h}_Y, -1]^T \tag{7}$$

Because the vertical axis of the land vehicle is more parallel to $\boldsymbol{n}_{\overline{\Sigma}}$, we use the surface $\overline{\Sigma}$ as the constraint surface in the following text. Furthermore, we limited the surface with the concept of a *Restricted Gradient Curve Surface*.

Definition 3.1 (Restricted Gradient Curve Surface):

A curve surface $\overline{\Sigma}_{\varepsilon_0}$ is called ε_0-*Restricted Gradient Curve*, if

$$\begin{aligned} &\forall \quad P({}^{W}X, {}^{W}Y, {}^{W}Z) \in \overline{\Sigma}_{\varepsilon_0} \ , \\ &\exists \quad \left|\frac{\partial {}^{W}Z}{\partial {}^{W}X}\right|^2 + \left|\frac{\partial {}^{W}Z}{\partial {}^{W}Y}\right|^2 < \varepsilon_0^2 \end{aligned} \tag{8}$$

where $\varepsilon_0 > 0$ could be easily confined by the general construction standards of highways. So, we identify all smooth ground surfaces $\overline{\Sigma}$ with ε_0-*Restricted Gradient Curve Surface* in the following text.

Definition 3.2 (Ideal Driving Trace):

A curved line $\Gamma \subset \overline{\Sigma}$ is called an *Ideal Driving Trace*, if the normal plane, Π_P^{Γ}, is also perpendicular to Λ at any point P on Γ , where Λ is the center line of road lane. And the distance from P to Λ is a constant $0 < \delta < W/2$, where the W is the width of road lane.

Assuming that $Q \in \overline{\Sigma}$ is a point in road lane, there are also two definitions as follows:

The plane Π_Q^{Γ} is called a normal plane of Γ relative to point Q, if Π_Q^{Γ} is a normal plane of Γ and $Q \in \Pi_Q^{\Gamma}$.

Vector $\boldsymbol{l}_{\Gamma}(Q)$ is called unit tangent vector of Γ relative to point Q, if $\boldsymbol{l}_{\Gamma}(Q) \perp \Pi_Q^{\Gamma}$ and $\|\boldsymbol{l}_{\Gamma}(Q)\| = 1$.

B. The Statistic Constraints Between Moving Vehicle and Road

- **Lane Constraint**
  Generally, the driver must keep the land vehicle between lane boundaries.

Assume that the vehicle is driven fluctuating about an Ideal Driving Trace Γ, and its velocity is $v(t)$ at time t. The algebraic distance from O_B, the origin of vehicle frame, to Γ is $d(t)$ which is positive when O_B is leftward to Γ. The angle between driving velocity $v(t)$ and vector $\boldsymbol{l}_{\Gamma}(O_B)$ is $\psi(t)$ which counter-clockwise is positive. Especially, we represented vector $\boldsymbol{l}_{\Gamma}(O_B)$ as ${}^{C}\boldsymbol{l}_{\Gamma}(t)$ at time t in the camera frame.

Driving on a highway, generally, the angle $\psi(t)$ is restricted to a narrow field, and the sideslip angle between driving velocity $v(t)$ and vector $\boldsymbol{i}_B$ is negligible relative to $\psi(t)$. So, the angle between $\boldsymbol{l}_{\Gamma}(O_B)$ and $\boldsymbol{i}_B$ is identified as the same with $\psi(t)$ in the following text.

Assume that, the delay time of driver active could be neglected. So, the *Lane Constraint* could be predigest as the following dynamic[10]

$$\begin{cases} \dot{d}(t) = v(t)\cdot\sin(\psi(t)) \approx v(t)\cdot\psi(t) \\ \dot{\psi}(t) = -\lambda_1\cdot d(t) - \lambda_2\cdot\dot{d}(t) + u(t) \end{cases} \tag{9}$$

where $\lambda_1 > 0$ and $\lambda_2 > 0$ are the gains of driver-vehicle system respective to trace offset $d(t)$ and trace offset rate $\dot{d}(t)$, and $u(t)$ is a stationary white Gaussian noise with auto correlation function $R_{uu} = q\delta(\tau)$.

As the speed response time of the vehicle is far greater than sampling interval, we consider that the velocity of vehicle is a constant in this process, that is $v(t) = v$. Then formula (9) could be rewritten as a linear time-invariant system

$$\psi(t) = L[u(t)] \tag{10}$$

and the expectation of $\psi(t)$ is

$$E\{\psi(t)\} = L[E\{u(t)\}] = 0 \tag{11}$$

The state-space equation of the system (10) is

$$\begin{aligned} \dot{\mathbf{x}} &= \mathbf{A}\mathbf{x} + \mathbf{B}u(t) \\ \psi(t) &= C\mathbf{x} \end{aligned} \tag{12}$$

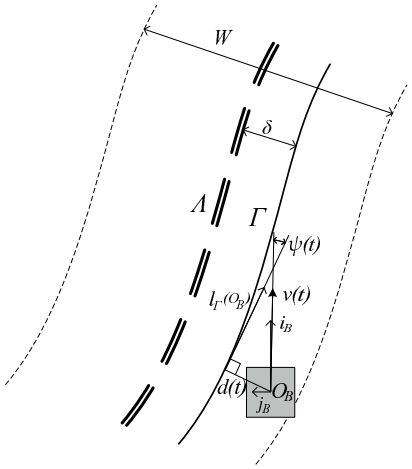

Fig. 2. Sketch map about Lane Constraint

where

$$\mathbf{x}=\begin{bmatrix} d(t) \\ \psi(t) \end{bmatrix}, \mathbf{A}=\begin{bmatrix} 0 & v \\ -\lambda_1 & -\lambda_2 v \end{bmatrix}, \\ \mathbf{B}=\begin{bmatrix} 0 \\ 1 \end{bmatrix}, \mathbf{C}=\begin{bmatrix} 0 & 1 \end{bmatrix} \quad . \tag{13}$$

Then, we could obtain the transfer function

$$\begin{aligned} G(s) &= C(sI-A)^{-1}B \\ &= \frac{s}{s^2+(\lambda_2 v)s+\lambda_1 v} \end{aligned} \tag{14}$$

and impulse response function

$$\begin{aligned} h(t) &= L[\delta(t)] \\ &= \mathscr{L}^{-1}[G(s)] \\ &= \frac{1}{b-a}\left(be^{-bt}-ae^{-at}\right)U(t) \quad , \end{aligned} \tag{15}$$

where

$$\begin{aligned} &\lambda_2^2 v^2 - 4\lambda_1 v > 0, \\ &a = \frac{\lambda_2 v + \sqrt{\lambda_2^2 v^2 - 4\lambda_1 v}}{2} > 0, \\ &b = \frac{\lambda_2 v - \sqrt{\lambda_2^2 v^2 - 4\lambda_1 v}}{2} > 0. \end{aligned} \tag{16}$$

And then obtain the auto covariance of $\psi(t)$ as follows

$$\begin{aligned} C_{\psi\psi}(\tau) &= R_{\psi\psi}(\tau) \\ &= \frac{q}{2(b^2-a^2)}\left(ae^{-a\tau}-be^{-b\tau}\right) \\ &\xrightarrow[\tau\to\infty]{} 0 \quad . \end{aligned} \tag{17}$$

So, $\psi(t)$ is an ergodic process with zero mean value: that is

$$\frac{1}{2T}\int_{-T}^{T}\psi(t,\xi)dt \xrightarrow[T\to\infty]{a.e.} E\{\psi(t)\}=0 \tag{18}$$

Furthermore, as mentioned above, the physical meaning of $\psi(t)$ is the angle between ${}^C\boldsymbol{l}_\Gamma(t)$ and ${}^C\boldsymbol{i}_B$, so

$$\left\langle {}^C\overline{\boldsymbol{l}_\Gamma}(\xi), {}^C\boldsymbol{i}_B \right\rangle \xrightarrow[T\to\infty]{a.e.} \left\| {}^C\overline{\boldsymbol{l}_\Gamma} \right\| * \left\| {}^C\boldsymbol{i}_B \right\| \tag{19}$$

where ${}^C\overline{\boldsymbol{l}_\Gamma}(\xi)$ denote the time averaged ${}^C\boldsymbol{l}_\Gamma(t,\xi)$ in a single observation.

$${}^C\overline{\boldsymbol{l}_\Gamma}(\xi)=\frac{1}{2T}\int_{-T}^{T}{}^C\boldsymbol{l}_\Gamma(t,\xi)dt \tag{20}$$

The equation (19) indicates that the orientations of ${}^C\overline{\boldsymbol{l}_\Gamma}(\xi)$ and ${}^C\boldsymbol{i}_B$ are parallel with probability 1, when $T\to\infty$. As a result, for a large sample number N, we could estimate ${}^C\overline{\boldsymbol{l}_\Gamma}(\xi)$ by the sample average

$${}^C\hat{\overline{\boldsymbol{l}_\Gamma}}(\xi)=\frac{1}{N}\sum_{i=1}^{N}{}^C\boldsymbol{l}_\Gamma(i,\xi) \quad . \tag{21}$$

- **Road Surface Constraint**
  As a fact that the vehicle must running on ground, the axis ${}^B Z$ of reference coordinate and the normal vector of surface $\overline{\Sigma}$ at local position are parallel, that is

$$\begin{aligned} &\left\langle {}^W\boldsymbol{k}_B(t), {}^W\boldsymbol{n}\left({}^W X_{(t)}, {}^W Y_{(t)}\right)\right\rangle \\ &= \left\| {}^W\boldsymbol{k}_B(t)\right\| * \left\| {}^W\boldsymbol{n}\left({}^W X_{(t)}, {}^W Y_{(t)}\right)\right\| \quad . \end{aligned} \tag{22}$$

- **The Hypothesis of Plentiful Vertical Line Segments in Vision Field**
  In this paper, a hypothesis is presumed that there are plentiful vertical line segments in the vision field on the highway, and the orientation of these line segments are approximate to vector k_W at local position participated of Gaussian noise with 0 mean and σ standard deviation.
- **The Distribution Hypothesis of Road Transverse Gradient**
  At time t, the road transverse of local position is denoted by $\varepsilon_\perp(t)$. We presume that the $\varepsilon_\perp(t)$ on selected highway is an ergodic process with $N(0,\sigma)$ distribution.

According to above constraints and hypotheses, the sidewise inclination of vehicle body $\varepsilon_j^B(t)$ is approximate to the road transverse gradient

$$\begin{aligned} \varepsilon_j^B(t) &= \left\langle {}^C\boldsymbol{j}_B, {}^C\boldsymbol{k}_W(t)\right\rangle \\ &= \left\langle {}^W\boldsymbol{j}_B(t), {}^W\boldsymbol{k}_W\right\rangle \\ &\approx \varepsilon_\perp(t) \quad . \end{aligned} \tag{23}$$

Consider that the $\psi(t)$ is not only a restricted small value but also an ergodic process with 0 mean, the difference between$\varepsilon_j^B(t)$ and $\varepsilon_\perp(t)$ is negligible. Of course the $\varepsilon_j^B(t)$ could be treated as an ergodic process, that is

$$\begin{aligned} \left\langle {}^C\boldsymbol{j}_B, {}^C\overline{\boldsymbol{k}}_W(\xi)\right\rangle &= \frac{1}{2T}\int_{-T}^{T}\varepsilon_j^B(t,\xi)dt \\ &\xrightarrow[T\to\infty]{a.e.} E\{\varepsilon_j^B(t)\}=0 \quad , \end{aligned} \tag{24}$$

where ${}^C\overline{\boldsymbol{k}}_W(\xi)$ denote the time average of ${}^C\boldsymbol{k}_W(t,\xi)$, the observed vertical vector of world frame.

$${}^C\overline{\boldsymbol{k}}_W(\xi)=\frac{1}{2T}\int_{-T}^{T}{}^C\boldsymbol{k}_W(t,\xi)dt \quad . \tag{25}$$

The formula (24) state that ${}^C\overline{\boldsymbol{k}}_W(\xi)$ and ${}^C\boldsymbol{j}_B$ are perpendicular each other with the probability 1, when $T\to\infty$. And so, for a

large sample number N, we could estimate ${}^{C}\bar{\boldsymbol{k}}_W(\xi)$ by simple average

$$ {}^{C}\hat{\bar{\boldsymbol{k}}}_W(\xi) = \frac{1}{N}\sum_{i=1}^{N} {}^{C}\boldsymbol{k}_W(i,\xi) \quad . \tag{26} $$

Note that although most real highway circumstances could satisfy the constraints and hypotheses mentioned above, there are still a few situations that would not satisfy the *Hypothesis of Plentiful Vertical Line Segments in the Vision Field* and the *Distribution Hypothesis of Road Transverse Gradient*. Therefore, the application scene must be well selected before using the method suggested in this paper.

C. Estimate the Rotation Matrix

To estimate the camera rotation matrix relative to the vehicle body by formula (4), the statistic relationships between frame vectors ${}^{C}\boldsymbol{i}_B$, ${}^{C}\boldsymbol{j}_B$ and scene features ${}^{C}\boldsymbol{l}_\Gamma(t,\xi)$, ${}^{C}\boldsymbol{k}_W(t,\xi)$ are discussed in formulas (19) and (24), which may be reduced further to the following equations:

$$ {}^{C}\hat{\boldsymbol{i}}_B = \frac{{}^{C}\hat{\bar{\boldsymbol{l}}}_\Gamma(\xi)}{\left\| {}^{C}\hat{\bar{\boldsymbol{l}}}_\Gamma(\xi) \right\|} \tag{27a} $$

$$ {}^{C}\hat{\boldsymbol{j}}_B = \frac{{}^{C}\hat{\bar{\boldsymbol{l}}}_\Gamma(\xi) \times {}^{C}\hat{\bar{\boldsymbol{k}}}_W(\xi)}{\left\| {}^{C}\hat{\bar{\boldsymbol{l}}}_\Gamma(\xi) \times {}^{C}\hat{\bar{\boldsymbol{k}}}_W(\xi) \right\|} \tag{27b} $$

$$ {}^{C}\hat{\boldsymbol{k}}_B = {}^{C}\hat{\boldsymbol{i}}_B \times {}^{C}\hat{\boldsymbol{j}}_B \tag{27c} $$

So, if the sample vectors ${}^{C}\boldsymbol{l}_\Gamma(i,\xi)$ and ${}^{C}\boldsymbol{k}_W(i,\xi)$ have been detected by the vision method[11][12][13], then the rotation matrix in formula (4) could be obtained easily by equations (21), (26) and (27a-27c).

IV. Experimental Results

To validate the performance of our algorithms with respect to all of the noise, we calibrated rotation parameters of the on-board camera in various real scenes. The videos were captured using a PULNIX TMC-9700 camera mounted on our prototype vehicle, Springrobot. Its image resolution is 384×216. It has constant internal parameters $u_0 = 258.7, v_0 = 81.6, \alpha = 625.6, \beta = 596.6$ and $\gamma = 0$, which is calibrated by Zhang's method[14].

Fig. 3. Two typical re-calibration images in different real scenes

The samples ${}^{C}\boldsymbol{l}_\Gamma(i,\xi)$ and ${}^{C}\boldsymbol{k}_W(i,\xi)$ of each frame were extracted by a method combining Collins's[11] and Lutton's[13]. Figure3 shows some typical images captured from these road videos. The Statistical Vanishing Points were estimated from these images and from the previous, where the Vanishing Point associate with ${}^{C}\hat{\bar{\boldsymbol{l}}}_\Gamma(\xi)$ was shown as a light square and ${}^{C}\hat{\bar{\boldsymbol{k}}}_W(\xi)$ was out of the image.

A. Estimation of the Statistical Vanishing Points

A working video frame set was found using the current frame and the N-1 previous ones. The tangents of the road boundary image at the close end in these frames were clustered into a group, and the edge segments of vertical line segments were clustered into the other group. For each group, we represented the line segments as normals of the associated great circles on the Gaussian sphere. The Vanishing Point Estimation problem fell well within the domain of direction statistics[11][15][16].

B. Rotation Matrix Calibration

The vectors from the origin point of the Gaussian sphere pointing toward these vanishing points were just what we needed to determine the vectors associated with Inherent Vanishing Points in formulas (27a)(27b) and (27c), ${}^{C}\boldsymbol{l}_\Gamma(i,\xi)$ and ${}^{C}\boldsymbol{k}_W(i,\xi)$. Then the rotation matrix ${}^{C}_{B}\mathscr{R}$ could be derived from formula (4). At last, we could obtain the Euler angles as follows:

$$ \begin{cases} \phi = \arccos {}^{C}_{B}\mathscr{R}_{33} \\ \psi = \arctan \dfrac{{}^{C}_{B}\mathscr{R}_{23}}{{}^{C}_{B}\mathscr{R}_{13}} \\ \theta = -\arctan \dfrac{{}^{C}_{B}\mathscr{R}_{32}}{{}^{C}_{B}\mathscr{R}_{31}} \end{cases} \tag{28} $$

TableI shows the mean and σ standard deviation of the estimated Euler angles in various scenes. As is clear, the results are stable after about 90 calibration frames in different scenes. We also note that there is a little uncertainty about $\sigma < 0.0025$ that could hardly be decreased. It is acceptable in application.

Zhang's flexible calibration method[14] has been used to obtain the contrasted data in the static calibration field, in which frontage is defined by gingerly driving the vehicle along a 50m straight line. TableII shows contrasted calibration results in different static calibration fields.

It's clear that there is obvious uncertainty in the results uncertainty between different calibration fields. As we mentioned in sectionI, the angle ψ has a standard deviation of about 0.0222 that will lead to a great reconstruction error when a far vision distance is considered.

V. Conclusion

For resolving the extrinsic parameter of an on-board camera dynamically, we suggested to treat the *essential vanishing points* of the on-board camera as the invariable visual cues, which are invisible but accessible. As shown throughout the paper, this is motivated by the fact that such cues naturally enclose the rotation matrix describing the coordinate frame associated with vehicle in the coordinate system with the on-board camera. In most conditions, statistically, the tangents of the road boundaries beside the position of vehicle are coherent with the vehicle orientation and the natural vertical edges perpendicular to the lateral axis of

TABLE I

RESULTS WITH TWO REAL SCENES OF 90 TROUGH 270 VIDEO FRAMES

		after 90 frames		after 150 frames		after 210 frames		after 270 frames	
		Eular ang.	σ	Eular ang.	σ	Eular ang.	σ	Eular ang.	σ
scene1	ϕ	1.5804	0.0008	1.5806	0.0007	1.5807	0.0006	1.5810	0.0005
	ψ	-0.0292	0.0019	-0.0293	0.0018	-0.0295	0.0017	-0.0296	0.0016
	θ	1.5843	0.0024	1.5834	0.0019	1.5835	0.0016	1.5836	0.0014
scene2	ϕ	1.5809	0.0009	1.5809	0.0008	1.5811	0.0007	1.5815	0.0006
	ψ	-0.0296	0.0002	-0.0295	0.0001	-0.0296	0.0001	-0.0297	0.0002
	θ	1.5794	0.0015	1.5788	0.0014	1.5789	0.0012	1.5790	0.0010

TABLE II

CONTRAST RESULTS DERIVED IN DIFFERENT STATIC CALIBRATION FIELDS

	Eular ang. in field 1	Eular ang. in field 2	Eular ang. in field 3	Eular ang. in field 4	σ
ϕ	1.5728	1.5934	1.5749	1.5681	0.0096
ψ	-0.0260	-0.0396	0.0202	-0.0131	0.0222
θ	1.6018	1.6120	1.5986	1.6173	0.0075

vehicle. This information is enough to determine the so-called *essential vanishing points* and the rotation matrix. We have shown that there exist compact and efficient algorithms to compute very accurate solutions online. Algorithms have been tested on real scene data online. Our approach shows the convenience and dependability in the scenes that met our simple restriction.

REFERENCES

[1] S. Ernst, C. Stiller, J. Goldbeck, and C. Roessig, "Camera calibration for lane and obstacle detection," in *Proc. IEEE/IEEJ/JSAI International Conf. Intelligent Transportation Systems, 1999*, 5-8 Oct. 1999, pp. 356–361.

[2] L. Wang and W. Tsai, "Camera calibration by vanishing lines for 3-d computer vision," *Pattern Analysis and Machine Intelligence, IEEE Transactions on*, vol. 13, no. 4, pp. 370–376, 1991.

[3] T. Bucher, "Measurement of distance height in images based on easy attainable calibration parameters," pp. 314–319, 3-5 Oct. 2000.

[4] F. Wang, "A simple and analytical procedure for calibrating extrinsic camera parameters," *Robtics and Automation, IEEE Transaction on*, vol. 20, no. 1, pp. 121–124, 2004.

[5] J. Liu, "The effect of aerodynamics characteristic on automobile driving stability," *Journal of Xi'an Highway University*, vol. 119, no. 11, pp. 86–88, 1999.

[6] F. Wang, "Aerodynamics of road vehicles," *Annual Review of Fluid Mechanics*, vol. 25, pp. 485–537, 1993.

[7] L. Ma, N. Zheng, Q. Li, and H. Cheng, "Dynamic approach of camera auto-calibration for vision system on autonomous vehicle," vol. 39, no. 10, pp. 1072–1076, 2005.

[8] J. Craig, *Introduction to Robtics: Mechanics and Control*, 2nd ed. Addison-Wesley, 1989.

[9] D. Forsyth and J. Ponce, *Computer Vision: A modern Approach*. The Pearson Education, Inc., Prentice Hall, Inc., 2003.

[10] K. Feng, "Vehicle lateral control for driver assistance and automated driving," PhD thesis, Engineering-Mechanical Engineering in the Graduate Division, Univ. of California, Berkeley, Berkeley, California, Spring 2000.

[11] R. Collins and R. Weiss, "Vanishing point calculation as a statistical inference on the unit sphere," in *Proc. International Conf. Computer Vision, 1990*, 4-7 Dec. 1990, pp. 400–403.

[12] G. McLean and D. Kotturi, "Vanishing point detection by line clustering," *Pattern Analysis and Machine Intelligence, IEEE Transactions on*, vol. 17, no. 11, pp. 1090–1094, 1995.

[13] E. Lutton, H. Maitre, and J. Lopez-Krahe, "Contribution to the determination of vanishing points using hough transform," *Pattern Analysis and Machine Intelligence, IEEE Transactions on*, vol. 16, no. 4, pp. 430–438, 1994.

[14] Z. Zhang, "A flexible new technipue for camera calibration," *Pattern Analysis and Machine Intelligence, IEEE Transactions on*, vol. 22, no. 11, pp. 1330–1334, 2000.

[15] P. Jupp and K. Mardia, "A unified view of the theory of directional statistics, 1975-1988," *International Statistical Review*, vol. 57, pp. 261–294, 1989.

[16] K. Mardia, *Statistics of Directional Data*. New York: Academic Press, 1972.